Diyala Journal for Pure Science

Surface Topography and Optical Properties for (MgOx-1ZnSx) Thin Films Prepared by Chemical Spray Pyrolysis.

Hussein S. Al-Rikabi[1], M. H. AL-TIMIMI[1], Ahmed Hamed Abed[2] and W. H. ALBANDA[3]

[1] Physics Department – College of Science – Diyala University, Diyala, Iraq.
[2]The General Directorate for Education in Diyala, Diyala, Iraq.
[3]Science Department - College of Basic Education – Al Mustansiriya University, Iraq.

sciphyms2104@uodiyala.edu.iq

Received: 14 June 2022 **Accepted: 17 July 2022**

DOI: https://dx.doi.org/10.24237/djps.1804.607D

Abstract

Pure and doped magnesium oxide (MgO) thin films were prepared with different volumetric ratios (0, 2, 4, 6, and 8%) of zinc sulfide (ZnS) on glass substrates at (350 °C) by chemical spray pyrolysis technique. The surface topography, absorption spectrum, absorption coefficient and Urbach energy of the prepared films were studied. The atomic force microscopy (AFM) results revealed that the surface topography of the prepared films changes as the percentage of doping with zinc sulfide (ZnS) increases. The absorbance spectrometry of the prepared films was measured by UV-vis. The Urbach energy of the prepared thin films increased by increasing the doping ratios with (ZnS).

Keywords: Thin film, MgO, ZnS, Surface Topography, Urbach Energy.

Diyala Journal for Pure Science

Surface Topography and Optical Properties for (MgOx-1ZnSx) Thin Films Prepared by Chemical Spray Pyrolysis.

Hussein S. Al-Rikabi, M. H. AL-TIMIMI, Ahmed Hamed. Abed and W. H. ALBANDA

طبوغرافيا السطح والخواص البصرية للأغشية الرقيقة (MgOx-1ZnSx) المحضرة بواسطة الانحلال الكيميائي الحراري

حسين صبحي عبدالرحمن[1]، محمد حميد عبدالله[1]، احمد حامد عبد[2] ووداد هنو عباس[3]

[1] قسم الفيزياء – كلية العلوم – جامعة ديالى، ديالى، العراق
[2] المديرية العامة للتربية في ديالى، ديالى، العراق
[3] قسم العلوم - كلية التربية الأساسية - الجامعة المستنصرية، العراق

الخلاصة

تم تحضير أغشية أكسيد المغنيسيوم النقي الرقيقة (MgO) والمشوب بنسب حجمية مختلفة (0، 2، 4، 6، 8)٪ من كبريتيد الزنك (ZnS) على ركائز زجاجية عند (350 °C) بتقنية التحلل الكيميائي الحراري. تمت دراسة طبوغرافية السطح وطيف الامتصاصية ومعامل الامتصاص وطاقة اورباخ للأغشية المحضرة. أظهرت نتائج فحص مجهر القوة الذرية (AFM) أن طبوغرافية السطحية للأغشية المحضرة تتغير مع زيادة نسبة التشويب بكبريتيد الزنك (ZnS). تم قياس مطياف الامتصاصية للأغشية المحضرة بواسطة (UV-vis). زادت طاقة اورباخ للأغشية الرقيقة المحضرة بزيادة نسب التشويب بـ (ZnS).

الكلمات المفتاحية: الأغشية الرقيقة، MgO، ZnS، طبوغرافيا السطح، طاقة اورباخ.

Introduction

Thin MgO films have an important scientific and technological role due to their application properties [1]. Magnesium oxide (MgO) thin films are used in several applications, including electronic devices, solar cells, LEDs, and sensors [1-3]. (MgO) has a wide bandgap and remarkable chemical and thermal stability [1, 2]. In general, dopants are useful for significantly modifying the properties of host materials. Several doping have been used to modify the properties of MgO thin films, such as (Zn, Ag, Cr, Al, Fe) [4-8]. In the current study, we chose zinc sulfide (ZnS) as the doping component because (ZnS) is a low-toxicity, low-cost, and readily available substance [9]. Moreover, (ZnS) is a composite (II-VI) semiconductor; it has a high refractive index and bandgap (3.72 eV at room temperature) and is used in many different technological applications [10]. Thin (MgO) films can be deposited by various techniques, including electron beam evaporation [4, 11], (sol-gel) [12], spraying [5], chemical vapor deposition (CVD) [13], spin coating [14], spray pyrolysis technology [15, 16], etc. The spray pyrolysis technique, compared to the previous techniques, is simple in cost and can deposit films in a large area [17, 18]. In the current work, the surface topography, absorbance, and urbach energy of the thin (MgO) films pure and doped with (ZnS) were studied using the spray pyrolysis technique.

Experimental part

Magnesium oxide (MgO) pure thin films and doped with zinc sulfide (ZnS) were prepared on glass substrates at (350 °C) by spray pyrolysis. (0.1M) of magnesium chloride ($MgCl_2.6H_2O$) was used to get (MgO) and (0.1M) of Zinc nitrate hexahydrate ($Zn(NO_3).6H_2O$) and (0.1M) of thiourea (CH_4N_2S) to get (ZnS) all dissolved in distilled water . Thin (MgO) films pure and doped were obtained with different volumetric ratios (0, 2, 4, 6, and 8%) of (ZnS) after spraying the solution with a compressor at (1.5 bar) on glass substrates. The surface topography properties were measured using an atomic force microscope (AFM), absorbance, absorption coefficient, and urbach energy using (UV-vis) for all the prepared films.

Results and Discussion

(XRD) Analysis

Fig. 1 shows the (XRD) patterns of pure magnesium oxide (MgO) and doped with zinc sulfide. The diagnostic peaks (Characteristic Peaks) showed that pure magnesium oxide (MgO) was obtained with a cubic crystal structure (F23 no.196) with crystalline dimensions (a=b = c = 4.22 Å) and angles (α=β=γ= 90°). As shown in Fig. 1a, which matches the Standard Pattern (JCPDS 01-074-1225). From Fig. 1b, we notice that the process of doping with zinc sulfide (ZnS) led to a decrease in the intensity (Low Intensity) and an increase in the width of the diagnostic peaks with an increase in the percentage of doping, This is due to the substitution of (Mg) ions with sulfur and zinc ions (Zn^{+2} and S^{-2} ions), the diffusion of ions within the crystal lattice of magnesium oxide (MgO) [19, 20], and the emergence of new peaks of low intensity after the doping process at the corners (2Θ= 28.7°, 47.56°, 56.38°) for the (002) (110) (112) crystalline levels, indicating the formation of a hexagonal (ZnS) Crystal Structure (P63mc no.186) with crystalline dimensions (a=b = 3.82 Å, c = 6.25 Å) and angles (α=β=90°, γ=120°), which corresponds to standard spectrum (JCPDS 00-002-1310).

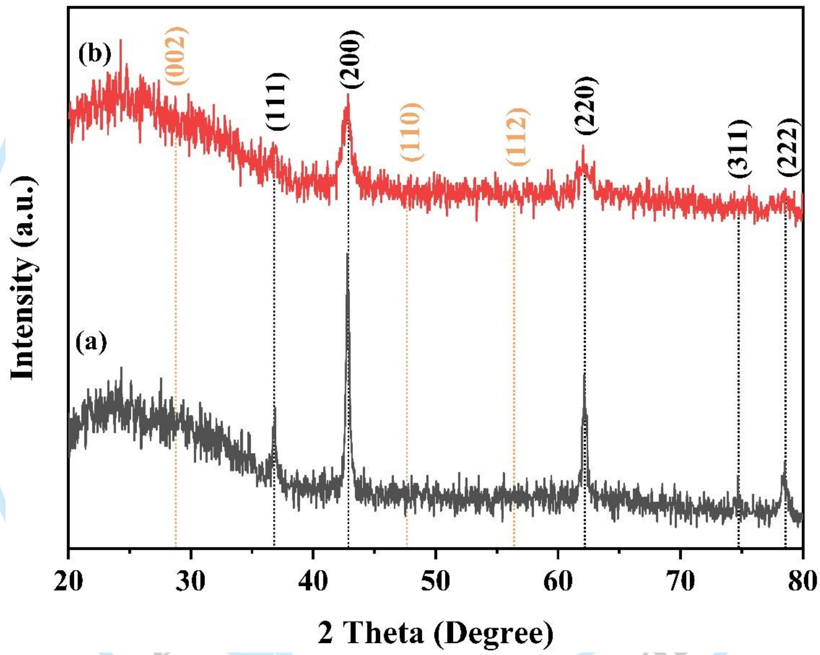

Figure 1: X-ray diffraction patterns of thin film (MgO) pure and doped with zinc sulfide (ZnS) films, a- (MgO) Pure, b- 8% (ZnS)

Surface Topography

Fig. 2 shows the images of the results of the atomic force microscope (AFM) tests for all the prepared films. The topography of the thin (MgO) films was studied and doped with different volumetric ratios (0,2,4,6, and 8%) of (ZnS) using atomic force microscopy (AFM).

The (AFM) images indicated that the surface morphology strongly depends on the doping concentration in the prepared thin films. The values of (Roughness Average) and root mean square of roughness (RMS) values decrease for all the prepared films except for the ($MgO_{0.98}ZnS_{0.02}$) film, as it was noticed that the roughness values and (RMS) values increased, the values of the grain size rate decrease with the increase of the percentage of doping with sulfide Zinc (ZnS) for all prepared films. This is consistent with the study [21], except for the film ($MgO0._{92}ZnS_{0.08}$). An increase in the rate of grain size was observed. The increase in the average grain size is probably due to the occupancy of the ZnS atoms in interstitial lattice positions and inter-grain regions [22].

The decrease in surface roughness is due to the reduction of the average crystalline size of (MgO) films after (ZnS) replacement [23-25]. This means that the square root of the mean roughness square and the surface roughness are directly proportional to the crystalline size. Also, the more extensive grain formation may lead to a decrease in surface roughness [26]. Table 1. shows the surface roughness and particle size values with an increasing percentage of doping with (ZnS).

Table 1: Roughness and (RMS) for the prepared thin films.

Samples	Roughness Average Sa (nm)	RMS (nm)	Grain Size (nm)
MgO	16.94	25.02	27.87
$MgO_{0.98}ZnS_{0.02}$	33.41	42.71	26.29
$MgO_{0.96}ZnS_{0.04}$	10.91	12.69	14.19
$MgO_{0.94}ZnS_{0.06}$	4.922	6.037	5.04
$MgO_{0.92}ZnS_{0.08}$	9.641	12.59	21.25

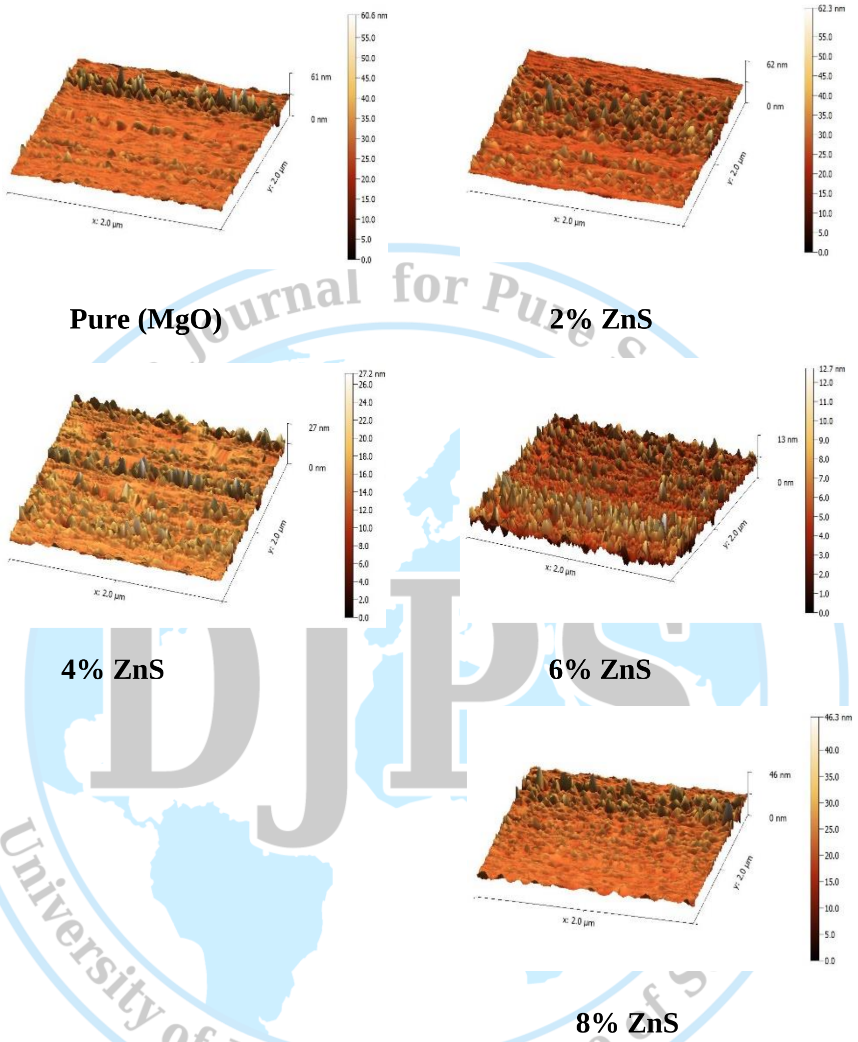

Figure 2: AFM images for the prepared thin films

Absorbance and Absorption Coefficient

Fig. 3 shows the absorbance values for all the prepared films. We notice that when doping (MgO) films with different percentages (0, 2, 4, 6, and 8%) of zinc sulfide (ZnS), the absorbance values increase with the increase in the percentage of doping (ZnS) [27], and this is due to the entry of the atoms of the material the impurity within the crystalline structure of the prepared films, which results in the formation of local levels between the valence band and the conduction band, which in turn leads to the absorption of photons with low energies. This is what corresponds to the highest absorption [28]. Fig. 4. shows the change of the absorption coefficient of all the prepared films as a function of the energy of the incident photon, where the absorption coefficient was calculated for all films prepared at a base temperature (350 °C) through the relationship (1) [29-31], and we note that the value of the absorption coefficient for all films ($\alpha > 10^4$ cm^{-1}), This confirms the occurrence of direct electronic transmissions [32-34]. The absorption coefficient of the prepared films increases with the increase in the percentage of doping with zinc sulfide (ZnS), The reason for this increase is that the process of doping with zinc sulfide (ZnS) created secondary levels within the energy gap, which increased the process of low-energy electronic transitions between the valence band and the level of impurities in addition to the normal transitions between energy bands, and this led to an increase in the absorption process of the incident photons and thus a rapid increase in the value of the absorption coefficient [35, 36]. $\alpha=2.303A/t$ (1)

(A) and (t) represents the film's absorbance and thickness.

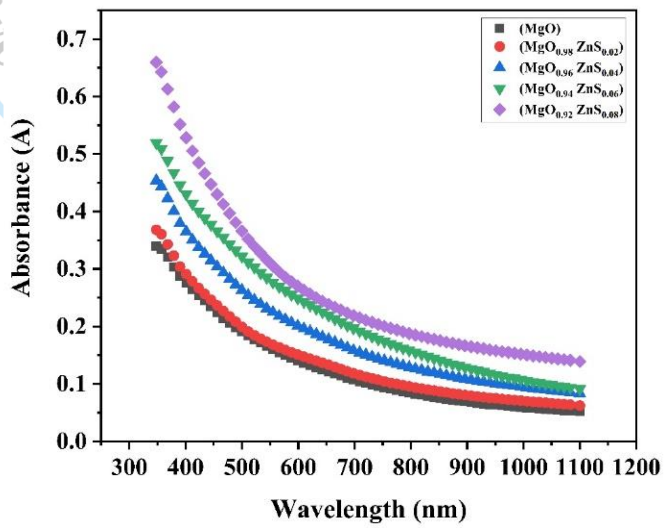

Figure 3: Absorbance as a function of the wavelength of the prepared films.

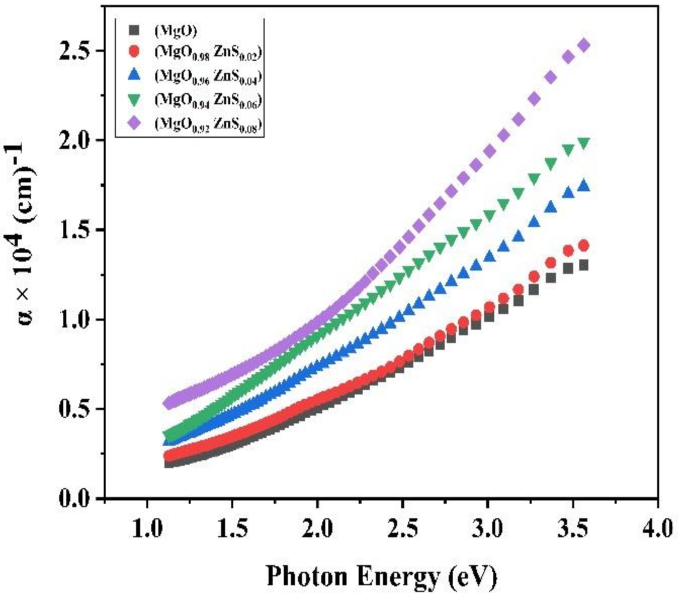

Figure 4: Absorption Coefficient of the prepared films.

Urbach Energy

Fig. 5 shows the graph relationship between the photon energy (hυ) and the logarithm of the absorption coefficient (Ln(α)) for all the prepared films.

The reciprocal of the slope of the straight line represents the energy values of the Urbach tails for the prepared films. Fig. 6 shows the values of Urbach energy as a function of the percentage of doping with zinc sulfide (ZnS), where we note that its value increases with the increase in the percentage of doping, which is consistent with the results reached by the researcher [37]. The increase in the energy values of Urbach tails is attributed to the increase in the number of local energy levels in the optical energy gap, and thus the energy of Urbach tails increases [8].

Diyala Journal for Pure Science

Surface Topography and Optical Properties for (MgOx-1ZnSx) Thin Films Prepared by Chemical Spray Pyrolysis.

Hussein S. Al-Rikabi, M. H. AL-TIMIMI, Ahmed Hamed. Abed and W. H. ALBANDA

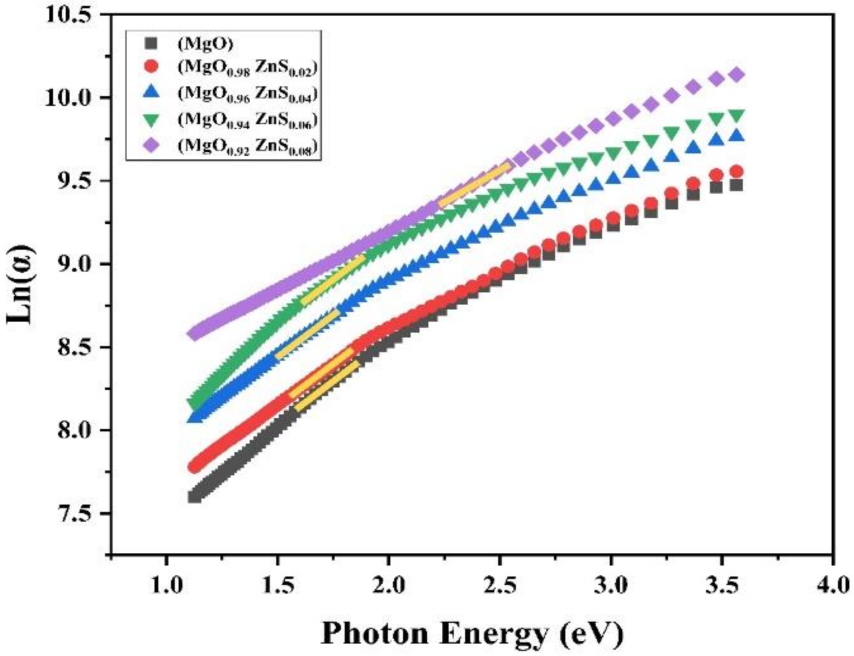

Figure 5: The relationship between (hυ) and (Ln (α)) of the prepared films

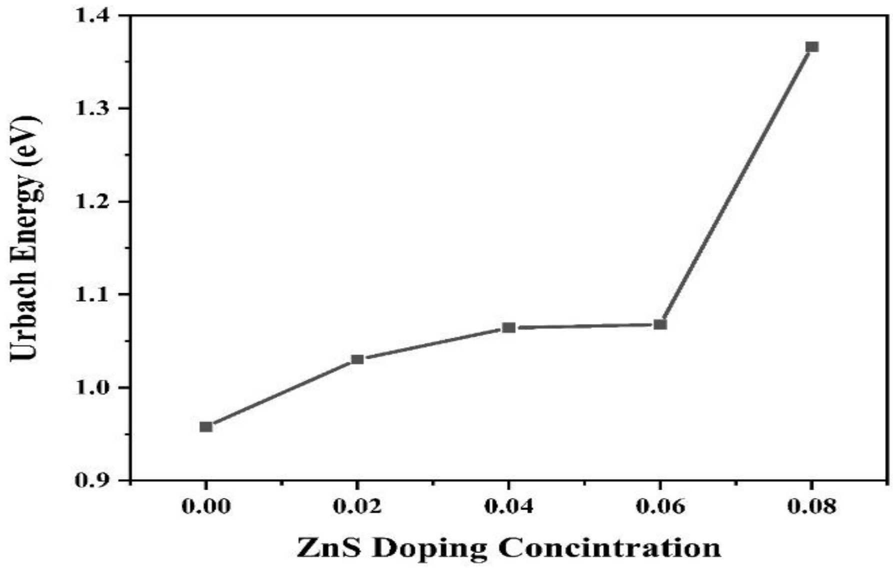

Figure 6: Urbach energy values as a function of doping ratios.

Surface Topography and Optical Properties for (MgOx-1ZnSx) Thin Films Prepared by Chemical Spray Pyrolysis.

Hussein S. Al-Rikabi, M. H. AL-TIMIMI, Ahmed Hamed. Abed and W. H. ALBANDA

Conclusions

X-ray diffraction assay showed the successful fabrication of the prepared thin films. The results of atomic force microscopy (AFM) show that the surface roughness rate of the prepared films decreases with an increasing percentage of doping with zinc sulfide (ZnS). Through UV-vis examination, the values of absorbance and absorption coefficient increased by increasing the percentage of doping with (ZnS). Also, the urbach energy increased with an increase in the percentage of doped with zinc sulfide (ZnS) within the range of (0.958-1.3663) eV.

References

1. G. Carta, N. El Habra, L. Crociani, G. Rossetto, P. Zanella, A. Zanella, G. Paolucci, D. Barreca, E. Tondello, Chemical vapor deposition,13(4),185-189(2007)
2. A. Moses Ezhil Raj, L. Nehru, M. Jayachandran, C. Sanjeeviraja, Crystal Research and Technology: Journal of Experimental and Industrial Crystallography, 42(9),867-875(2007)
3. S. Visweswaran, R. Venkatachalapathy, M. Haris, R. Murugesan, Journal of Materials Science: Materials in Electronics, 31(17), 14838-14850(2020)
4. H. K. Yu, Thin Solid Films, 653, 57-61(2018)
5. S. Benedetti, N. Nilius, S. Valeri, The Journal of Physical Chemistry C, 119, (45), 25469-25475(2015)
6. P. Maiti, P. S. Das, M. Bhattacharya, S. Mukherjee, B. Saha, A.K. Mullick, A.K. Mukhopadhyay, Materials Research Express, 4(8), 086405(2017)
7. M. R. Islam, M. Rahman, S. Farhad, J. Podder, Surfaces and Interfaces, 16, 120-126(2019)
8. M. G. M. Nion, M. H. Kabir, M. A. Mona, M. J. Haque, N. Shahariar, M. Hafiz, M. S. Rahman, Results in Materials, 12, 100235(2021)
9. A. Goktas, A. Tumbul, Z. Aba, A. Kilic, and F. Aslan, Optical Materials, 107, 110073(2020)
10. M. Ashokkumar, A. Boopathyraja, Superlattices and Microstructures, 113, 236-243(2018)

11. M. Saeed, M. Al-Timimi, O. Hussein, Digest Journal of Nanomaterials and Biostructures, 16(2), 563-569(2021)
12. I. C. Ho, Y. Xu, J. D. Mackenzie, Journal of Sol-Gel Science and Technology, 9(3), 295-301(1997)
13. T. K. Talukdar, S. Liu, Z. Zhang, F. Harwath, G. S. Girolami, J. R. Abelson, Journal of Vacuum Science & Technology A: Vacuum, Surfaces, and Films, 36 (5), 051504(2018)
14. T. Güngör, B. USLU, E. Güngör, A. BÖBREK, (2020)
15. M. Tlili, N. Jebbari, W. Naffouti, N. T. Kamoun, The European Physical Journal Plus, 135(8), 1-12(2020)
16. A. J. Mawat, M. H. AL-Timimi, Journal of The College of Basic Education, 27(113),(2021)
17. M. H. Kabir, A. Bhattacharjee, M. M. Islam, M. Rahman, M. Rahman, M. Khan, Journal of Materials Science: Materials in Electronics, 32(3), 3834-3842(2021)
18. M. H. Kabir, M. Rahman, M. Khan, Chinese Journal of Physics, 56(5),2275-2284(2018)
19. R. Kim, Y. Kim, Y.-U. Lee, H.-J. Kim, J.-W. Park, Surface and Coatings Technology, 161(1), 52-57(2002)
20. S. Gowrishankar, L. Balakrishnan, N. Gopalakrishnan, Ceramics International, 40(1), 2135-2142(2014)
21. A. M. El Sayed, Materials Research Express, 5(11), 116403(2018)
22. G. Turgut, Journal of Materials Science: Materials in Electronics,28(22), 16992-17001(2017)
23. C. Y. Tsay, H. C. Cheng, Y. T. Tung, W. H. Tuan, C. K. Lin, Thin Solid Films, 517(3), 1032-1036(2008)
24. T. Saidani, M. Zaabat, M. Aida, B. Boudine, Superlattices and Microstructures, 88, 315-322(2015)
25. M. Ajili, M. Castagné, N. K. Turki, Superlattices and Microstructures,53, 213-222(2013)
26. M. D. Sakhil, Z. M. Shaban, K. S. Sharba, N. F. Habub, K. H. Abass, S. S. Chiad, A. S. Alkelaby, NeuroQuantology, 18(5), 56(2020)
27. E. Parvizi, R. Tayebee, E. Koushki, Semiconductors, 53(13), 1769-1783(2019)
28. X. Liu, S. Chen, M. Li, X. Wang, Thin Solid Films, 515(17), 6744-6748(2007)

29. S. Liqa'G, H. S. Rasheed, M. H. Abdul-Allah, Diyala Journal For Pure Science, 8(3)-part 2,(2012)
30. M. Abdullal, R. Jaseen, A. H. Resan, J. Pure Sciences, 7(3), 205-213(2011)
31. D. Fakralden, S. Hamed, M. Abdul-Allah, Ibn AL-Haitham Journal For Pure and Applied Science, 24(1), (2016)
32. I. R. Agool, K. J. Kadhim, A. Hashim, International Journal of Plastics Technology, 21(2), 397-403(2017)
33. A. T. Abood, O. A. A. Hussein, M. H. Al-Timimi, M. Z. Abdullah, H. M. S. Al Aani, W. H. Albanda, Structural and optical properties of nanocrystalline SnO2 thin films growth by electron beam evaporation, in AIP Conference Proceedings, 2020, 2213(1), AIP Publishing LLC, p. 020036.
34. R. Ali, K. Sharba, M. Al-Timimi, K. Abass, N. Habubi, I. Al-Baidhany, S. Chiad, EasyChair, 2516-2314(2019)
35. A. Taşer, M. E. Güldüren, H. Güney, Materials Chemistry and Physics, 272, 124993(2021)
36. J. Al-Zanganawee, M. Al-Timimi, A. Pantazi, O. Brincoveanu, C. Moise, R. Mesterca, D. Balan, S. Iftimie, M. Enachescu, Journal of Ovonic Research,12(4), 201-207(2016)
37. F. T. Ibrahim, Iraqi Journal of Applied Physics, 13(3), (2017)